AIAA JOURNAL
Vol. 41, No. 10, October 2003

Analysis of Flow Conditions in Freejet Experiments for Studying Airfoil Self-Noise

Stéphane Moreau* and Manuel Henner†
Valeo Motors and Actuators, 78321 La Verrière, France
Gianluca Iaccarino‡ and Meng Wang§
Stanford University, Stanford, California 94305
and
Michel Roger¶
Ecole Centrale de Lyon, 69134 Ecully, France

A new set of mean wall pressure data has been collected on a controlled diffusion airfoil at a chord Reynolds number of 1.2×10^5 in a freejet anechoic wind tunnel. Comparisons of the experimental data with Reynolds-averaged Navier–Stokes (RANS) simulations in free air show significant flowfield and pressure loading differences, indicating substantial jet interference effects. To analyze these effects, a systematic RANS-based computational fluid dynamics study of the experimental flow conditions has been carried out, which quantifies the strong influence of the finite jet (nozzle) width on the aerodynamic loading and flow characteristics. When the jet width is not sufficiently large compared to the frontal wetted area of the airfoil, the airfoil pressure distribution is found to be closer to the distribution on a cascade than that of an isolated profile. The airfoil lift is significantly reduced. Accounting for the actual wind-tunnel setup recovers the wall pressure distribution on the airfoil without further empirical angle-of-attack corrections. These jet interference effects could be responsible for the discrepancies among some earlier experimental and computational studies of airfoil self-noise. They should be accounted for in future noise computations to ensure that the experimental flow conditions are simulated accurately.

I. Introduction

WHEN considering the sound emitted by a rotating machine such as an engine cooling fan, an airplane turbofan, or an air-conditioning unit, one significant contributor to the overall noise is the trailing-edge noise from the blades. It comes from the conversion of local flow perturbations in the boundary layer into acoustic waves through interaction with the acoustically thin trailing edge. Depending on the flow Reynolds number (based on the local chord length) and the geometry of the blade trailing edge, the acoustic scattering is associated with most of the broadband component and some narrower-band structures of the far-field acoustic spectrum.[1] The noise radiation is generally more severe for loaded blades, when flow separation occurs at the trailing edge. This mechanism also provides the minimum noise configuration of such machines when all interactions with their environment (turbulence ingestion and flow distortion at the inlet, rotor–stator interaction with downstream stationary components, etc.) are removed.[2,3] As another example, the same edge scattering mechanism constitutes an important source of wind-turbine noise.[4,5]

The study of trailing-edge noise or airfoil self-noise received much attention mainly in the late 1970s and early 1980s. It involved measurements of wall pressure fluctuation spectra and far-field acoustic spectra on two-dimensional mock-ups of various aerodynamic profiles in freejet anechoic wind tunnels.[6–8] The experimental data were then been used in the late 1990s to validate numerical prediction methods for trailing-edge aeroacoustics.[9–13] For typical engine cooling fan applications involving transitional and turbulent flows at Reynolds numbers of order 10^5, the numerical prediction requires information of the noise-generating eddies over a wide range of length scales. The traditional Reynolds-averaged Navier–Stokes (RANS) approach is insufficient. It needs to be substituted by the more expensive large-eddy simulations (LES) or combined with a suitable statistical model to yield the necessary unsteady surface pressure fluctuations and the near-field fluctuating Reynolds stresses, which provide the acoustic source functions. The radiated noise can then be computed using an aeroacoustic theory such as Ffowcs Williams and Hall's application[14] of Lighthill's analogy.

As with the application of any computational fluid dynamics (CFD) methods, the validity and accuracy of the solutions must be established first against known solutions or experimental measurements. This is particularly important in the case of aeroacoustic computation given the relatively small magnitude of noise signals. In the validation process, to have a valid comparison with experiments, the computation should reproduce as exactly as possible the experimental environment. In practice, however, simplified flow configurations are often employed in simulations. For instance, in all previous LES studies,[10,13] the airfoil has been assumed to be in a uniformly moving medium (free-air configuration). In contrast, most trailing-edge aeroacoustics experiments have been conducted in open-jet wind-tunnel facilities, where the airfoil is immersed in a jet downstream of the nozzle exit. The proximity of the airfoil to the jet nozzle exit and the limited jet width relative to the airfoil thickness and chord length can cause the airfoil pressure loading and flow characteristics to deviate significantly from those measured in free air and, hence, alter the radiated noise field.

The present work is aimed at quantifying these experimental installation effects as well as proposing more suitable experimental and numerical procedures. The characteristics of the previous experiments are first reviewed. They are then compared to new measurements collected in recent experiments at Ecole Centrale Lyon (ECL) on a cambered controlled diffusion (CD) airfoil developed at Valeo

Received 17 July 2002; revision received 5 February 2003; accepted for publication 5 April 2003.

*Senior Research Engineer and Research and Development Manager, Engine Cooling Fan Systems Core Competencies Group.
†Research Engineer, Engine Cooling Fan Systems Core Competencies Group.
‡Research Associate, Center for Turbulence Research. Member AIAA.
§Senior Research Scientist, Center for Turbulence Research. Member AIAA.
¶Professor, Laboratoire de Mécanique des Fluides et Acoustique.

Motors and Actuators. A systematic CFD study, based on RANS models, of flow conditions in the ECL experiment is carried out and compared with flows over an isolated airfoil in a uniform stream. The results shed some light on the fidelity of the flow conditions in the previous numerical simulations of trailing-edge experiments and provide guidance for the appropriate boundary conditions needed in future LES of such experiments.

II. Review of Experimental Setup and Data

To measure the pure airfoil self-noise, the aerodynamic profile must be placed in a large quiet environment and isolated as much as possible from the inlet duct providing the necessary airflow. Moreover, the inlet duct should have a low background noise and low residual turbulence (<1%), which explain the maximum outlet sections of about 0.5 m in most current test facilities. Finally, to avoid contamination of the acoustic signals by the flowfield, the airstream tube should be confined, away from the far-field microphones. All of the preceding criteria tend to show that an open freejet anechoic wind tunnel provides the best experimental compromise.

A. Previous Measurements

Two main sets of data have been reported previously on trailing-edge noise in freejet wind tunnels. In both experiments, two-dimensional airfoils are supported by side plates that are flush mounted to the nozzle lips.

In 1975, Blake measured the pressure and velocity fields near the trailing edge of a flat strut.[6] The latter, with a circular leading edge and an asymmetric beveled trailing edge, was placed in the nozzle wind tunnel flow at a 0-deg angle of attack. Several trailing-edge shapes and flow velocities were considered. In one of the measurements, the flow conditions were a freestream velocity of about 30 m/s and a Reynolds number based on the chord length Re_c of about 2.2×10^6. The geometry was chosen to produce a separated flow on the low-pressure side and an attached boundary layer on the high-pressure side. In this initial experiment, mean pressure was measured on the strut close to the trailing edge along with statistics of pressure and velocity fluctuations. Far-field acoustic data were later collected under different flow conditions with slightly modified trailing-edge geometry.[1] No account of possible inlet flow distortion was reported.

Later, in 1981, Brooks and Hodgson performed measurements on several NACA 0012 airfoils with various chord lengths and trailing-edge shapes.[7] The choice was motivated by the large amount of aerodynamic data available on this symmetric airfoil and the desire to study the difference between sharp and blunt trailing edges. By bolting the airfoil in three different positions in the side plates, three angles of attack with respect to the chord line, $\alpha_w = 0$, 5, and 10 deg, have been studied. The subscript w hereafter refers to the wind tunnel setup. The highest velocity achieved was a freestream velocity of 73.4 m/s, or a Reynolds number Re_c of about 3×10^6. Flush-mounted Kulite pressure transducers were used to measure the pressure fluctuations in the vicinity of the trailing edge. The acoustic radiation was measured simultaneously by eight microphones in the far field. The mean characteristics of the turbulent boundary layer at the trailing edge was obtained by a combination of a movable pitot rake and 14 Preston tubes. However, no direct measurements of wall pressure distribution have been reported in this experiment.

B. New ECL Measurements

Recently, measurements have been performed by Roger and Moreau[15] on both a NACA 0012 and a Valeo airfoil. The former is used to provide validation against the earlier experiment of Brooks and Hodgson.[7] The latter is a much thinner airfoil (about 4% thickness to chord ratio compared to 12% for the NACA 0012) with both blunt leading and trailing edges. It has been designed to achieve low drag by controlling the chordwise diffusion (CD airfoil). Moreover, the NACA 0012 is symmetric, whereas the Valeo airfoil is cambered with a camber angle of about 12 deg. The flow conditions for the CD airfoil are a freestream velocity V_0 of 16 m/s and a Reynolds number Re_c of about 1.2×10^5. The actual experimental setup, shown in Fig. 1, is comparable to that used by Brooks and Hodgson.[7] The geometric angle of attack can be continuously adjusted by two disks rotating inside the side plates around a zero reference aligned with the nozzle outflow.

Flush-mounted remote microphone probes (RMPs) on the airfoil[16] allow the measurements of both the mean wall static pressure and the fluctuating pressure spectra. Such probes are made with a spanwise flush-mounted capillary tube and a pin hole at the measuring point. The capillary is then progressively enlarged outside the mock-up till a small Electret microphone can be flush mounted. A long polyvinyl chloride tube is connected to the outer end of the capillary to attenuate longitudinal waves. Details of the technology and the calibration of the sensors may be found in Ref. 17. A movable

Fig. 1 Experimental setup with the Valeo profile in the ECL test facility.

Table 1 Characteristic dimensions in some airfoil self-noise experiments (in centimeters)

Airfoil	Chord c	Span s (c)	Airfoil thickness (w)	Nozzle–LE distance (c)	Jet width, w (c)
Flat strut	107.3	119.4 (1.11 c)	5.1 (0.02 w)		240 (2.24 c)
Blake[6]				−130	
Blake and Gershfeld[1]				∼10 (0.1 c)	
NACA 0012					
Brooks and Hodgson[7]	61	46 (0.75 c)	7.2 (0.24 w)	15 (0.25 c)	30 (0.49 c)
Roger	10	30 (3.00 c)	1.2 (0.09 w)	10 (1.00 c)	13 (1.30 c)
Valeo CD					
Roger (small wind tunnel)	13.6	30 (2.21 c)	0.5 (0.04 w)	10 (0.73 c)	13 (0.96 c)
Roger (large wind tunnel)	13.6	30 (2.21 c)	0.5 (0.01 w)	20 (1.47 c)	50 (3.68 c)

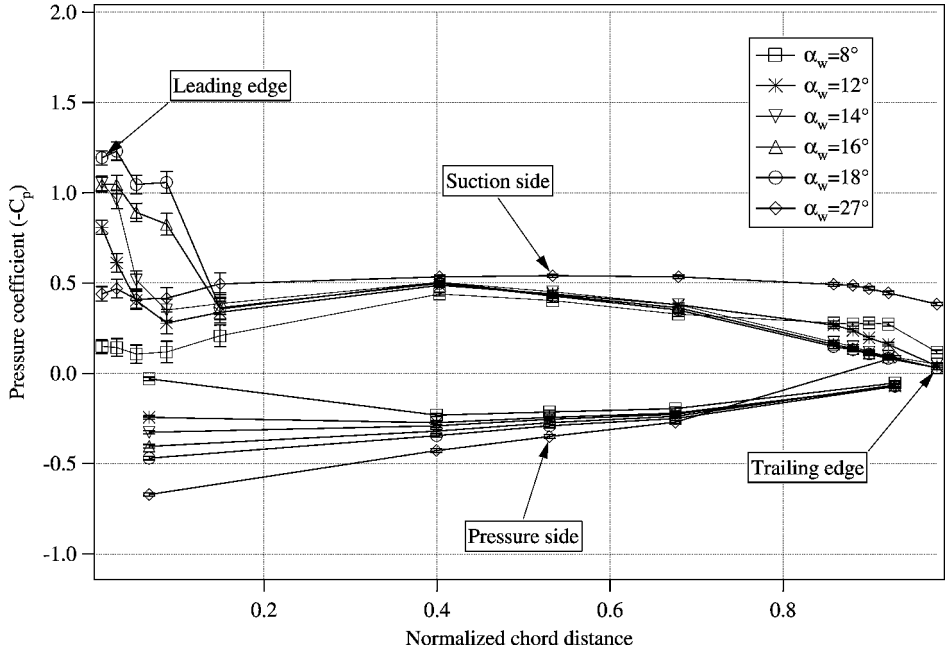

Fig. 2 Experimental pressure coefficient on the Valeo cambered CD profile.

microphone is placed in the far field to collect the acoustic spectra simultaneously. Finally, tuft visualizations are used to estimate qualitatively the flow separation zones, and a hot-wire rake is used to measure the wake velocity profile close to the trailing edge. The corresponding mean wall pressure measurements on the Valeo CD airfoil for five different geometric angles of attack are shown in Fig. 2. Good repeatability was achieved on this data set, and a maximum change of angle of attack of 0.5 deg causes a variation of 0.1 on the pressure coefficient. Note that, for $\alpha_w = 12$ deg, the flow is attached along the entire chord. At $\alpha_w = 14$ deg, the flow starts to separate near the trailing edge. This regime corresponds to turbulent vortex shedding with no mean backflow. Increasing the angle of attack to $\alpha_w = 16$ deg leads to a laminar recirculation zone near the leading edge. At $\alpha_w = 18$ deg, the separated zones, particularly the one near the leading edge, are increased in size. At much larger incidence ($\alpha_w = 27$ deg), the airfoil seems to be stalled with a recirculation bubble at the trailing edge, which is confirmed by a tuft survey along the chord.

C. Comparison of Experimental Dimensions

The various geometrical parameters involved in the described experiments are compared in Table 1. By examining the span-to-chord ratio s/c we can estimate the possible three-dimensionality effects induced by the side plates. Brooks and Hodgson's experiment[7] exhibits some three-dimensional influence as indicated by the nonuniform surface pressure spectra in Fig. 8 of Ref. 7. In contrast, the Roger et al. experiments are expected to be less affected at midspan where the RMPs are mounted. A comparison of the airfoil thickness and the jet width (or nozzle exit width) allows an estimate of the blockage induced by the airfoil in the jet. The latter is large in Brooks and Hodgson's experiment.[7] Moreover, data on jet boundary corrections for airfoil tests in open wind-tunnel jets[18] suggest that all experiments listed in Table 1 will yield significant differences between the actual angle of attack and the effective one, defined as the expected one in free air that would lead to the same lift distribution. The jet width also determines the extent of its potential core and, therefore, gives an estimate of the interaction of the shear layers generated at the nozzle lips with the airfoil surface. If a typical core length of four to five jet widths is assumed, by comparison with the airfoil chord length and thickness, it becomes clear that such an interaction may be present in Brooks and Hodgson's setup. Finally, the distance from the nozzle exit to the airfoil leading edge gives a hint at the potential interaction between the nozzle and airfoil and the consequent local modification of the effective angle of attack. These effects are irrelevant in Blake's experiment[6] because the airfoil is fully inside the jet nozzle (hence, the negative distance in Table 1) and the nozzle width is 48 times the airfoil thickness. However, they cannot be neglected in the experiment of Blake and Gershfeld.[1]

III. Numerical and Physical Models

A. Overall Formulation

As shown in Refs. 19 and 20, the aerodynamics of engine cooling fan systems in the blade reference frame involves essentially incompressible, transitional, or turbulent flows depending on the sections considered from hub (lower speed) to tip (higher speed). To account

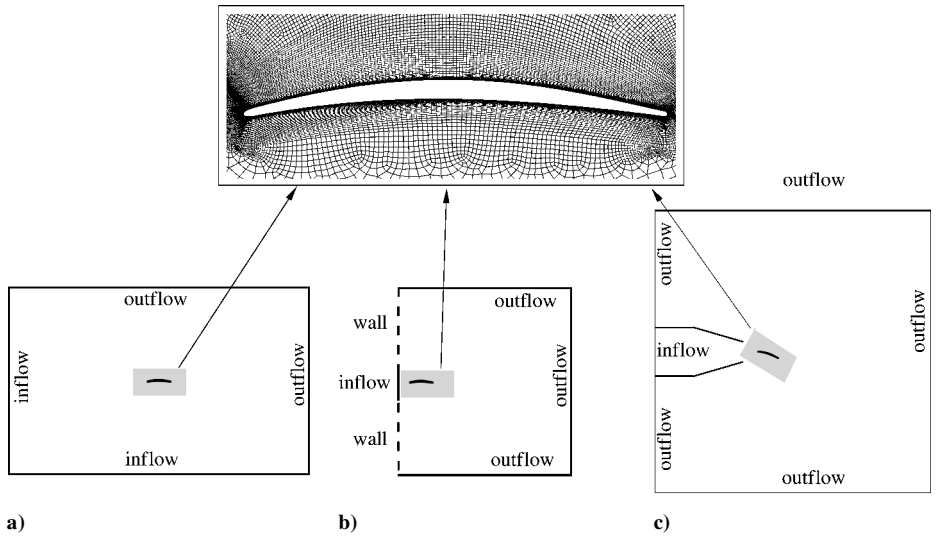

Fig. 3 Free-air and wind-tunnel topologies and boundary conditions.

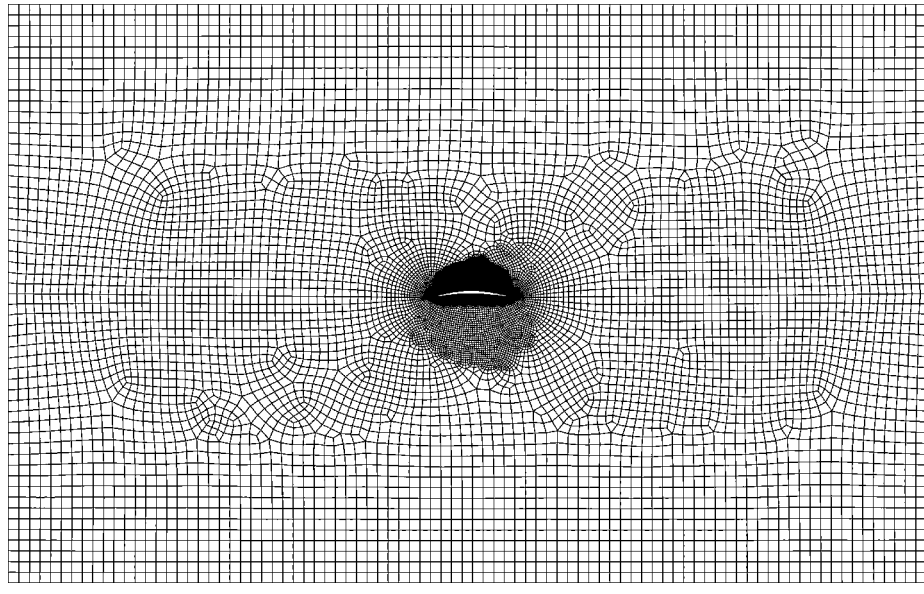

Fig. 4 Isolated airfoil unstructured fine grid.

for this usual environment, the flowfield has been modeled by the RANS equations with several two-equation turbulence models. At the solid boundaries, both wall functions and a two-layer approach have been used. The resulting set of conservative equations has been solved with either CFX-TASCflow 2.10 on multiblock structured grids or FLUENT 5.5 on unstructured grids. Details of the numerical schemes used for these computations and the corresponding validation test cases may be found in Ref. 20 for CFX-TASCflow and in Ref. 21 for FLUENT. The least diffusive second-order accurate schemes have always been used with both commercial codes. In the CFX-TASCflow simulations, four different turbulence models have been employed: the k–ε model with wall functions, the two-layer low-Reynolds-number k–ε model, the k–ω model, and Menter's shear stress transport (SST) model.[22] Only the v^2–f (variables as k, ε, or ω) (V2F) model[23] has been used with FLUENT. Previous comparisons with both codes using the same k–ε formulation led to very similar results for a cascade configuration of this CD airfoil, under the same flow conditions as in the current ECL tests.

To investigate the wind-tunnel installation effects, three flow configurations are considered in the numerical simulations. They include an isolated airfoil in free air (Fig. 3a), a simplified wind tunnel with finite jet width but no explicit account of the nozzle (Fig. 3b), and the so-called full wind tunnel, which includes the jet nozzle in the computational domain (Fig. 3c). All of the computations have been two dimensional as justified by the aspect ratio in Table 1.

B. Grid Analysis

The isolated airfoil simulations have been performed in a rectangular domain with about four chord lengths above and below the airfoil and six chord lengths upstream and downstream of the airfoil. To test the grid sensitivity of the solutions, a multiblock structured grid (66,000 cells) and two unstructured grids (30,000 and 55,000 cells) are employed. All of the grids have very similar clustering of points near the wall to capture the boundary layer properly (Fig. 4). Even though the unstructured fine grid has more points and is more regular chordwise at the leading edge, it has a smaller overall mesh size than the structured one because of the unstructured topology and grid adaptation based on the shear stresses. The solutions on all grids are very similar, and the wall pressure and friction distributions are seen to be grid and topology independent for each turbulence model studied. The corresponding results using the V2F model at a chord-referenced angle of attack $\alpha_i = 8$ deg are plotted in Figs. 5 and 6. The subscript i hereafter refers to the isolated airfoil flow conditions. On all grids, the dimensionless wall-normal grid spacing in wall units, Δy^+, is smaller than 1 over most of the chord length on both pressure and suction sides.

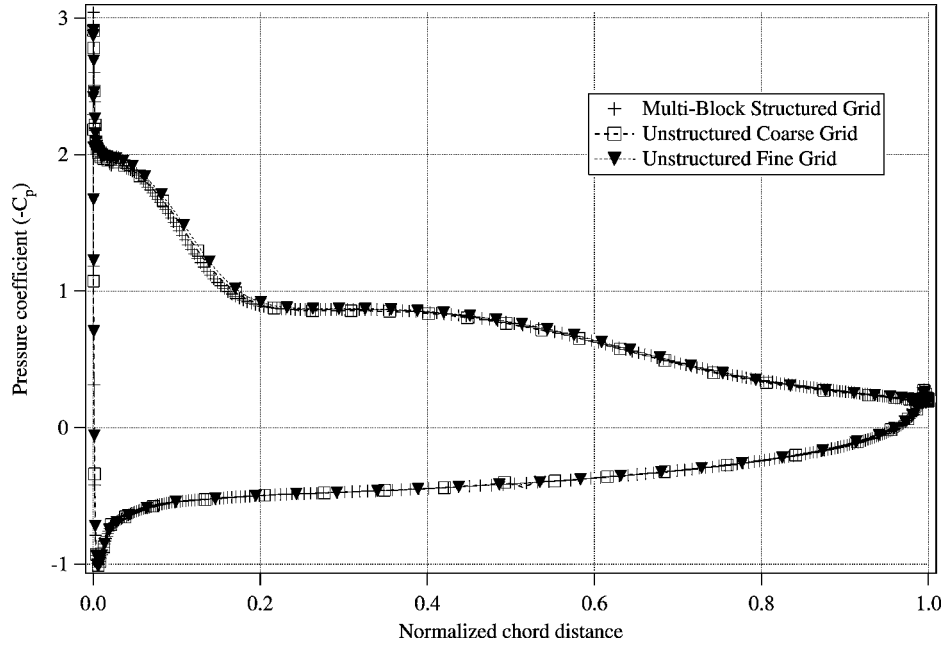

Fig. 5 Comparison of pressure coefficients on the CD profile computed on different grids.

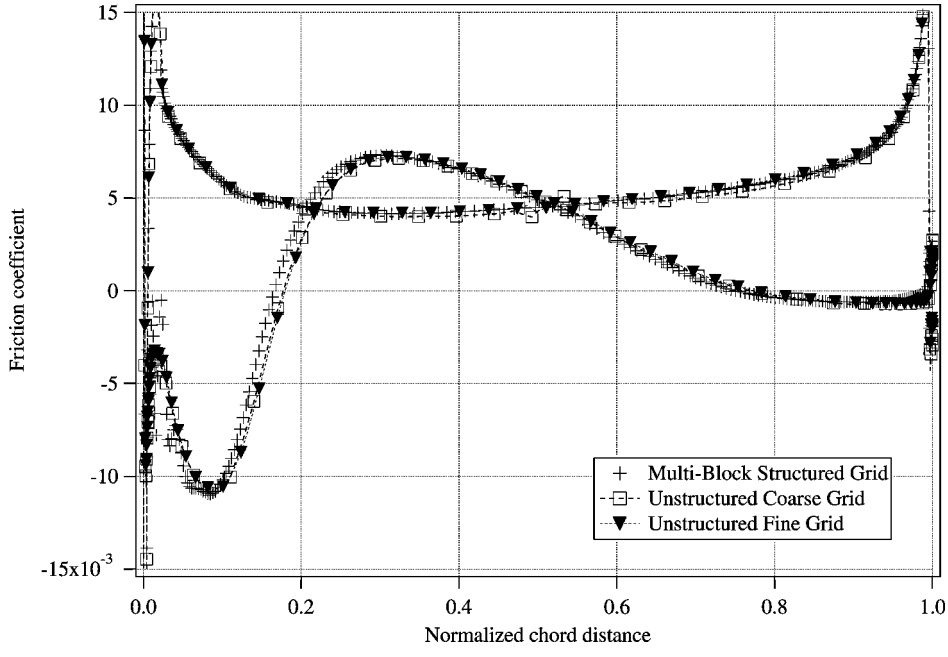

Fig. 6 Comparison of skin-friction coefficients on the CD profile computed on different grids.

In the simplified wind-tunnel simulations, the same grid density near the airfoil is used as shown in Fig. 3. The airfoil is placed closer to the left boundary according to the distance in Table 1. The computational box, shown in Fig. 3b is also extended farther away from the airfoil (1×1 m) to capture a wake deflection independent of the distant boundaries. The full wind-tunnel simulation also includes the complete nozzle geometry to assess the effect of the nozzle–airfoil interaction. The resulting grid is presented in Fig. 7.

C. Boundary Conditions

For the isolated airfoil, the incoming flow is assumed uniform and corresponds to the nozzle exit mean velocity. It is imposed at the left and bottom boundaries of the CFD domain. On the upper and right boundaries, an outlet pressure is applied. In the simplified wind-tunnel geometry, the inflow velocity is uniform within the nozzle width and is inclined with respect to the airfoil chord by the angle α_w. This simplified model allows a quick evaluation of the effect of the airfoil incidence on the same grid independently of the actual experimental setup, which is not always known precisely (particularly the center of rotation of the airfoil with respect to the nozzle). Yet, by rotating the jet instead of the mock-up, a small variation in the position of the airfoil within the jet core is introduced, which will mainly affect the pressure-side pressure distribution. The rest of the left boundary is a solid wall. On the upper and lower boundaries, an outlet pressure is imposed again. If the boundaries are sufficiently far from the jet, they should yield the same solutions. In the complete wind-tunnel simulations, the inlet boundary condition is set inside the nozzle and adjusted to provide a mean velocity of 16 m/s at the nozzle exit. The nozzle geometry and the relative position of the airfoil with respect to the nozzle are also exact.

D. Turbulence Modeling

The effect of different turbulence models has first been examined for the case of an isolated airfoil. Flow simulations have been

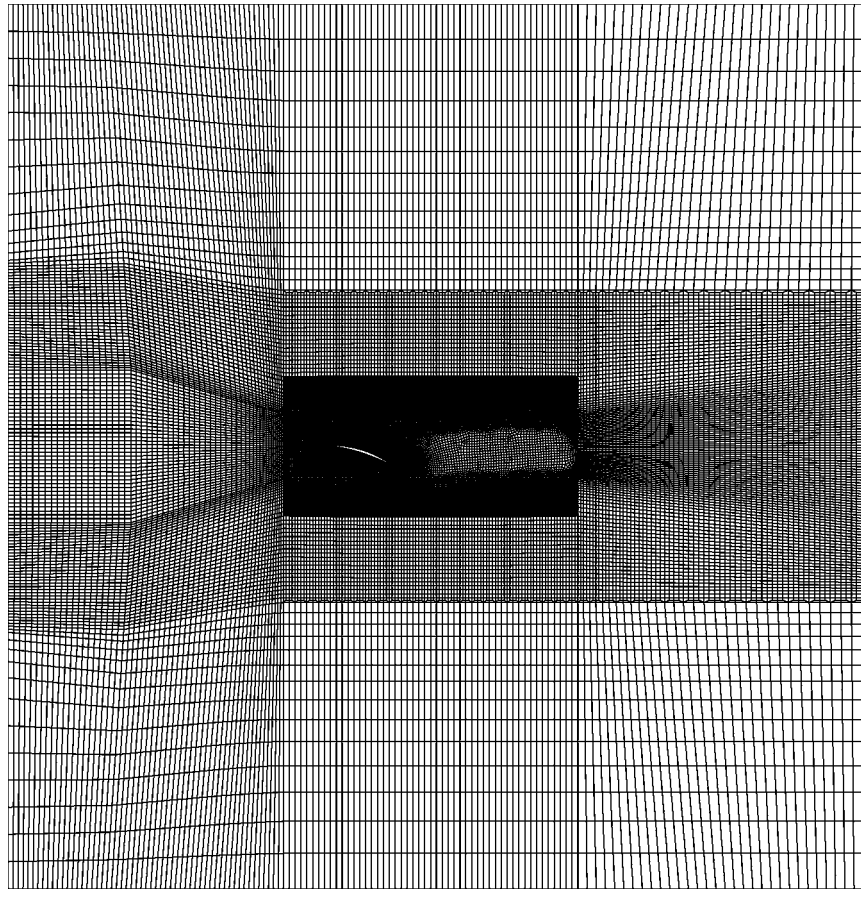

Fig. 7 Unstructured fine grid for the ECL wind tunnel.

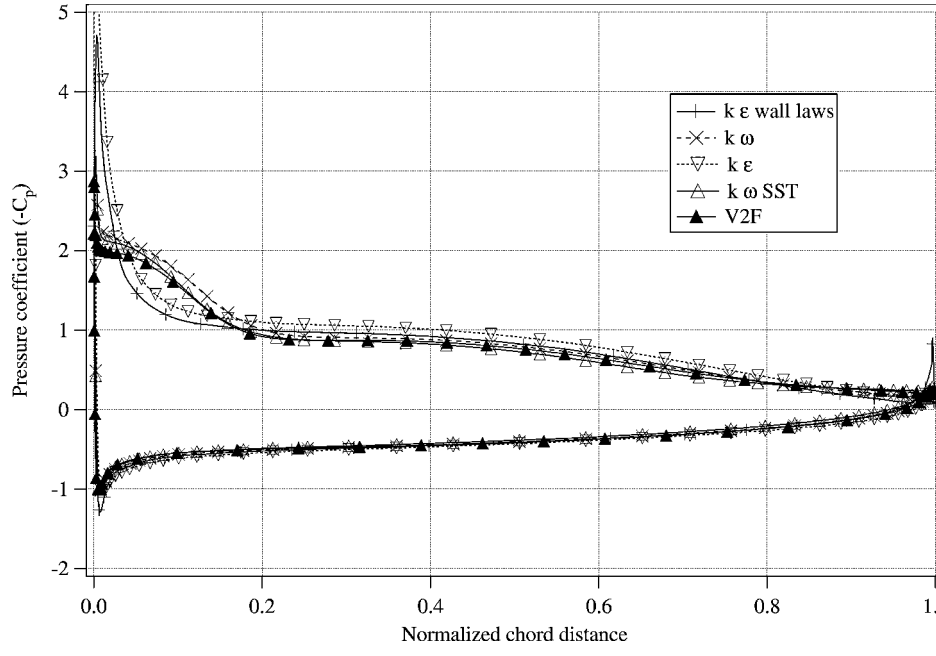

Fig. 8 Comparison of pressure coefficients on the CD profile in free air at $\alpha_i = 8$ deg, predicted using different turbulence models.

run for α_i between 0 and 10 deg with increments of 1 deg. All models agree at low angles of attack. At higher angles of attack (beyond 5 deg), two groups of results emerge. The two k–ε simulations predict no laminar flow separation at the leading edge and hardly any turbulent recirculation near the trailing edge. In contrast, the k–ω, SST, and V2F models predict increasing flow separations with α_i in both the trailing-edge and leading-edge regions, in agreement with experimental evidence (Fig. 2). The overall flow patterns are very similar to those reported by Winklemann and Barlow[24] or Bastedo and Mueller[25] on lifting surfaces in low-Reynolds-number flows. Figures 8 and 9 show the pressure and friction coefficients for $\alpha_i = 8$ deg. Figure 9 indicates that the largest turbulent recirculation zone is predicted by the SST model.

The different behavior at the leading edge of the k–ε model predictions can be traced to the overproduction of turbulent kinetic energy at the stagnation point, which prevents a local relaminarization of

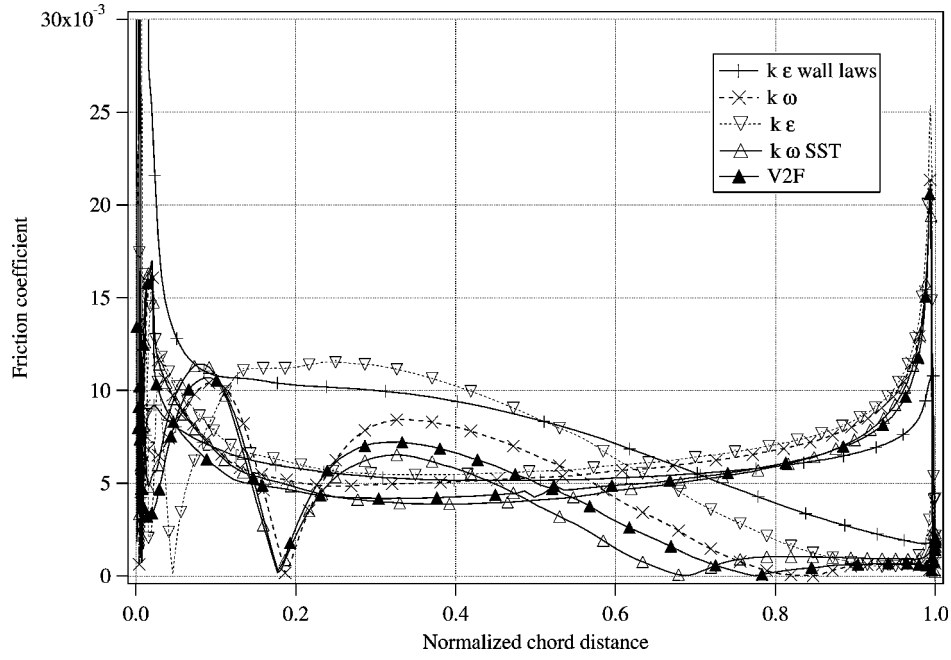

Fig. 9 Comparison of skin-friction coefficients on the CD profile in free air at $\alpha_i = 8$ deg, predicted using different turbulence models.

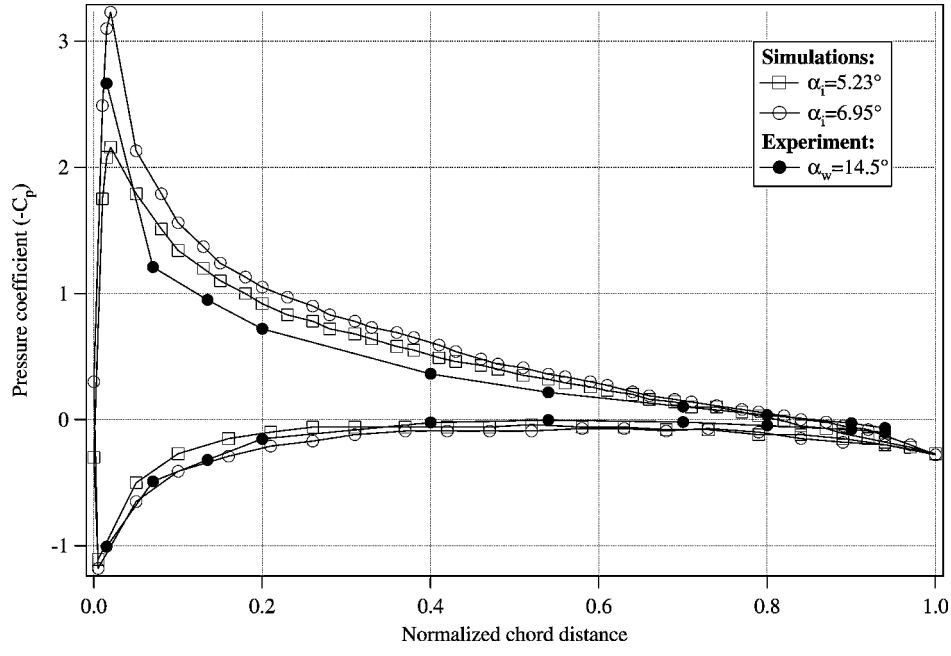

Fig. 10 Comparison of pressure coefficients on the NACA 0012 airfoil between isolated airfoil simulations and ECL test data.

the flow and, thus, the flow separation. This was also demonstrated in the cascade simulations reported in Ref. 26.

IV. Results

A. Isolated Airfoil Simulations

In Ref. 27, Brooks et al. found that the NACA 0012 airfoil in an open-jet tunnel could have the same loading as in free unbounded flow provided that a correction to the angle of attack was applied to account for the jet deflection. In the recent experiment at the ECL test facility with the same airfoil section, Roger (unpublished profile) found again a possible correction to the angle of attack as shown in Fig. 10. The correction is based on a comparison between the measured pressure coefficient distribution and a set of computed results in free air. In this case, the equivalent free-air angle of attack is found to be about $\alpha_i = 6$ deg for a wind-tunnel angle of attack $\alpha_w = 14.5$ deg, resulting in a correction of 8.5 deg. When the data in Table 1 are used, Eq. (2) of Ref. 27 yields a similar value, $\alpha_i = 5.3$ deg. Note that, although the integrated lift can be adjusted in this way, the precise distribution of pressure coefficient is not perfectly recovered, especially in the leading-edge area, indicating some installation effects in this experiment.

The same methodology has then been applied to the Valeo CD airfoil. However, as Fig. 11 shows, no correction on angle of attack could recover the experimental lift, which is much lower than the one computed in free air. Figure 11 shows the best qualitative comparison that can be achieved using angle-of-attack corrections of 8–9 deg. The CD airfoil seems to be far more sensitive to the installation effects than the NACA 0012 with a similar chord, which is most likely due to the difference in airfoil thicknesses and the camber of the CD airfoil.

Furthermore, Fig. 12 shows that the pressure levels obtained from the experiment relate quite well to the cascade loading obtained in previous simulations at Valeo. This suggests that the shear layers originating from the nozzle lips confine the flow in a manner similar

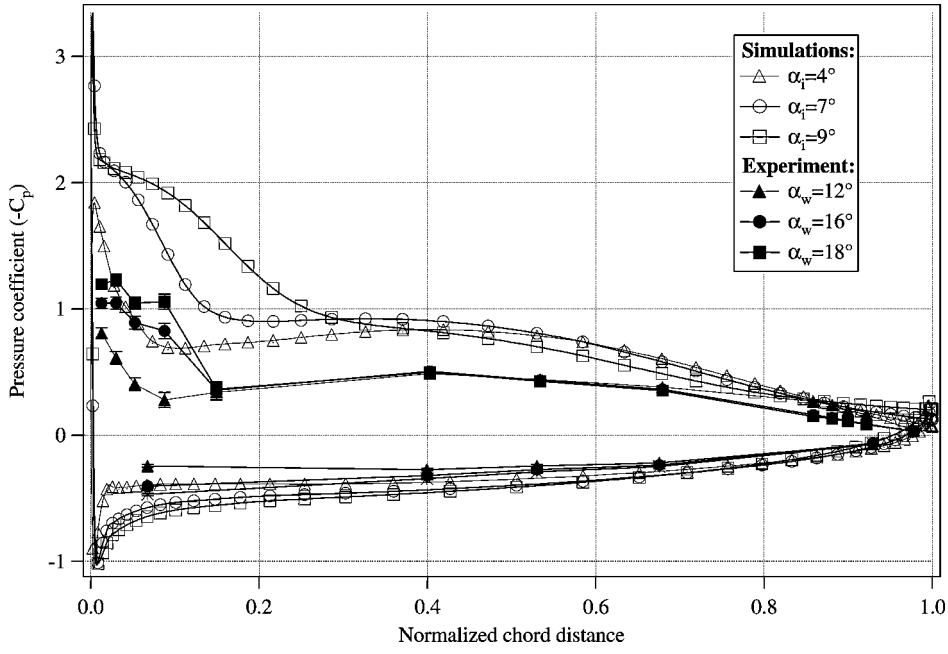

Fig. 11 Comparison of pressure coefficients on the CD airfoil between isolated airfoil simulations and ECL test data.

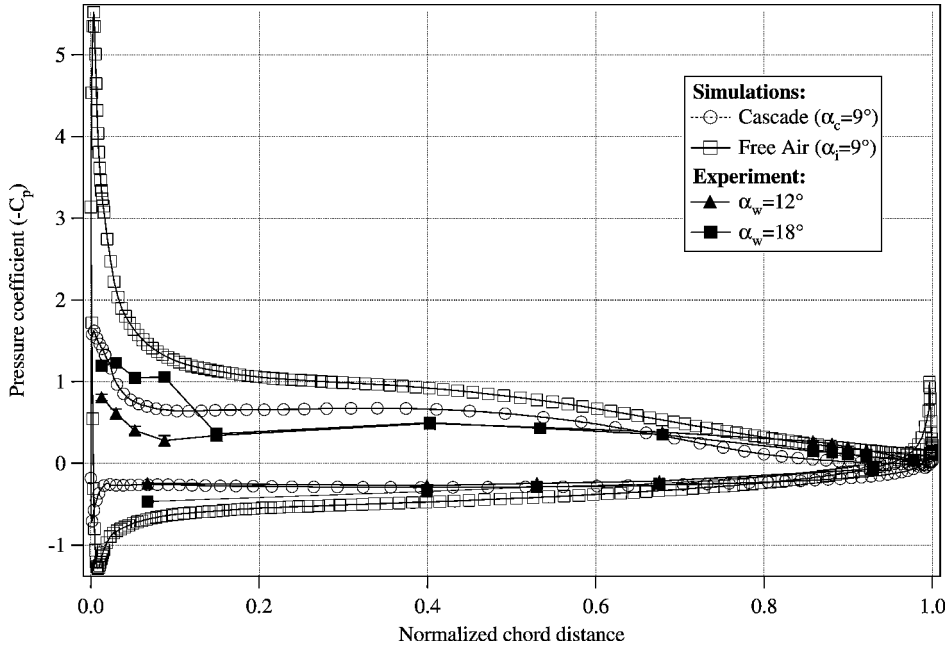

Fig. 12 Comparison of pressure coefficients on the CD airfoil between cascade and isolated airfoil simulations and ECL test data.

to a blade passage in a cascade (as will be seen clearly later). The large discrepancy between the ECL test data and free-air simulation results has motivated the following wind-tunnel simulations. Note that the large discrepancies between the boundary-layer momentum thickness found in Ref. 13 relative to that in Brooks and Hodgson's experiment[7] can most likely be attributed to this type of installation effects and the incorrect pressure gradients computed in free air compared to the actual ones in the open-jet experiments. Similar unsatisfactory pressure results have been reported in Fig. 5 of Ref. 12, although in Blake's experiment,[6] they are most likely attributed to other installation effects because the airfoil is inside the nozzle.

B. Simplified Wind-Tunnel Simulations

All wind-tunnel flow simulations presented here have been performed with the V2F model and a jet width of 13 cm. The initial focus is the simplified configuration whose geometry and boundary conditions were described earlier. Several angles of attack α_w have been considered in the current ECL setup corresponding to the experimental data in Fig. 2. Figure 13, compared with Fig. 11, clearly shows that the suction side pressure coefficient is now much better predicted, without further semi-empirical corrections. The laminar flow separation at high angle of attack ($\alpha_w = 18$ deg) is captured. Similar results are achieved with the k–ω and SST models as in Fig. 8 for the free-air case, which emphasizes the superiority of this set of turbulence models in predicting separated flow as compared to the k–ε model. The pressure levels on the pressure side are still quite different, especially close to the leading edge.

C. Full Wind-Tunnel Simulations

To address the latter problem and assess the effect of the simplified wind-tunnel model, a two-dimensional simulation of the full wind tunnel including the nozzle (compare Figs. 3 and 7) has been carried out, with the correct experimental position of the

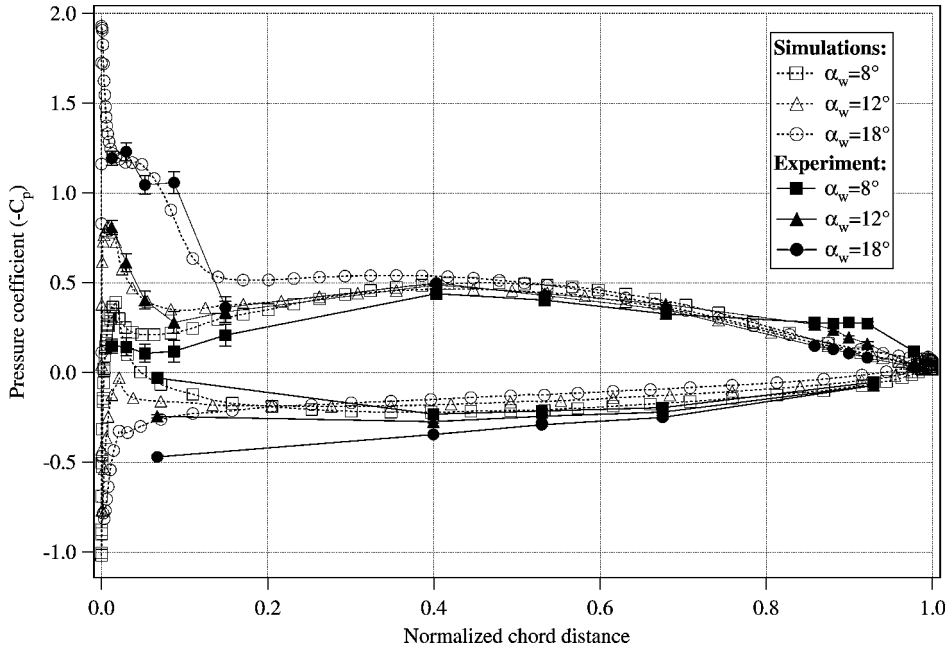

Fig. 13 Comparison of pressure coefficients on the CD airfoil between simplified wind-tunnel simulations and ECL test data.

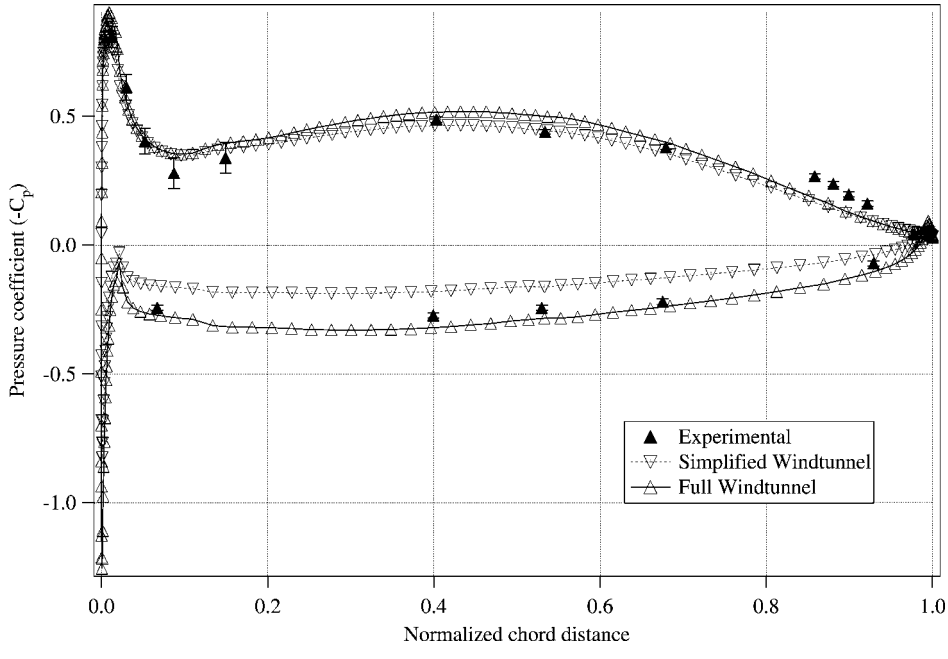

Fig. 14 Comparison of pressure coefficients on the CD airfoil at α_w = 12 deg between wind-tunnel simulations and ECL test data.

airfoil in the jet potential core. As shown in Fig. 14, for an angle of attack $\alpha_w = 12$ deg the pressure levels on the pressure side are nicely recovered. However no major change is found on the suction side: No flow separation is numerically predicted at the trailing edge. These remaining discrepancies seen at 10% of chord and, consequently, near the trailing edge are most likely caused by a transition to turbulence that occurs too early in the RANS simulations.

D. Jet Width Effect

With the large differences between the isolated airfoil case and the same airfoil in an open-jet acoustic tunnel established and explained, the influence of the jet width on the pressure and velocity distributions is now investigated. The motivation for this study is to provide guidance for the design of future experiments with minimal interference effects and for setting up the appropriate LES boundary conditions if such an interference is present. The simplified wind-tunnel model is used for this parametric study in which the jet width varies from 13 to 50 cm and the angle of attack $\alpha_w = 8$ deg.

Our calculations indicate that with a jet width at least twice as large as the current experimental value, most of the turbulent zone on the suction side is now very close to the free-air case. However at the leading edge, the wind-tunnel calculation does not show large laminar flow separation observed in the free-air case. To confirm these trends, an additional experiment has been dedicated in a larger wind tunnel available at ECL on the same CD airfoil mock-up at the same incidence with a jet width of 50 cm. The corresponding geometrical characteristics of this new setup is summarized in the last row of Table 1. As shown in Fig. 15, the measured pressure coefficient agrees with the simplified wind-tunnel simulation, as in the 13-cm case. The trailing-edge flow is even better predicted for the wider jet case. However, large discrepancies with the free-air case persist, which underlines the importance of accounting for the jet interference effect in aeroacoustic calculations. The good agreement

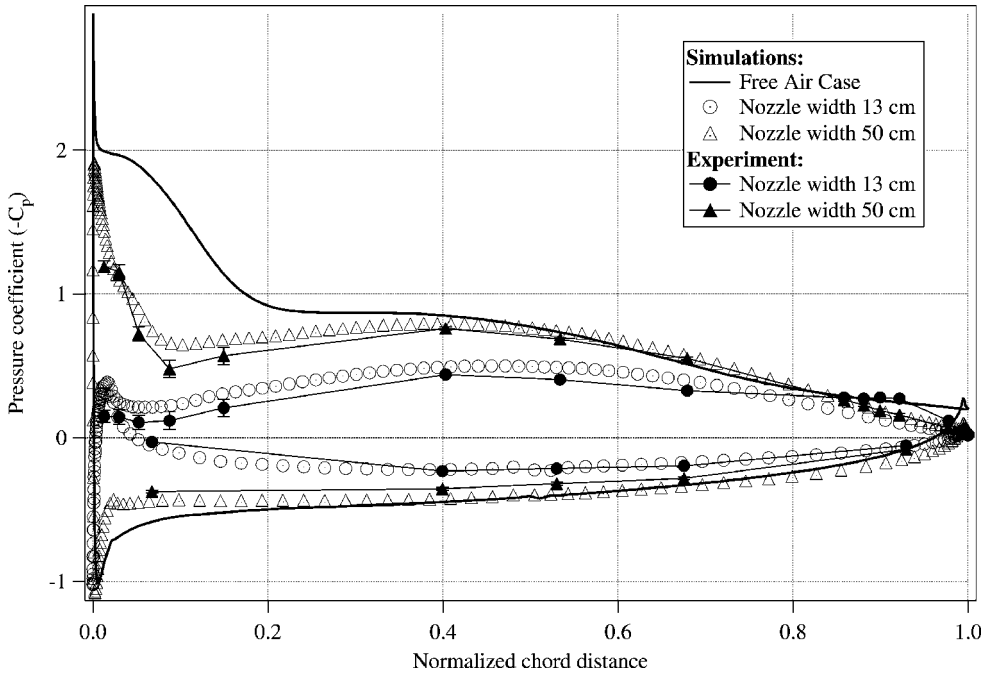

Fig. 15 Comparison of pressure coefficients on the CD airfoil at $\alpha_w = 8$ deg for different nozzle widths.

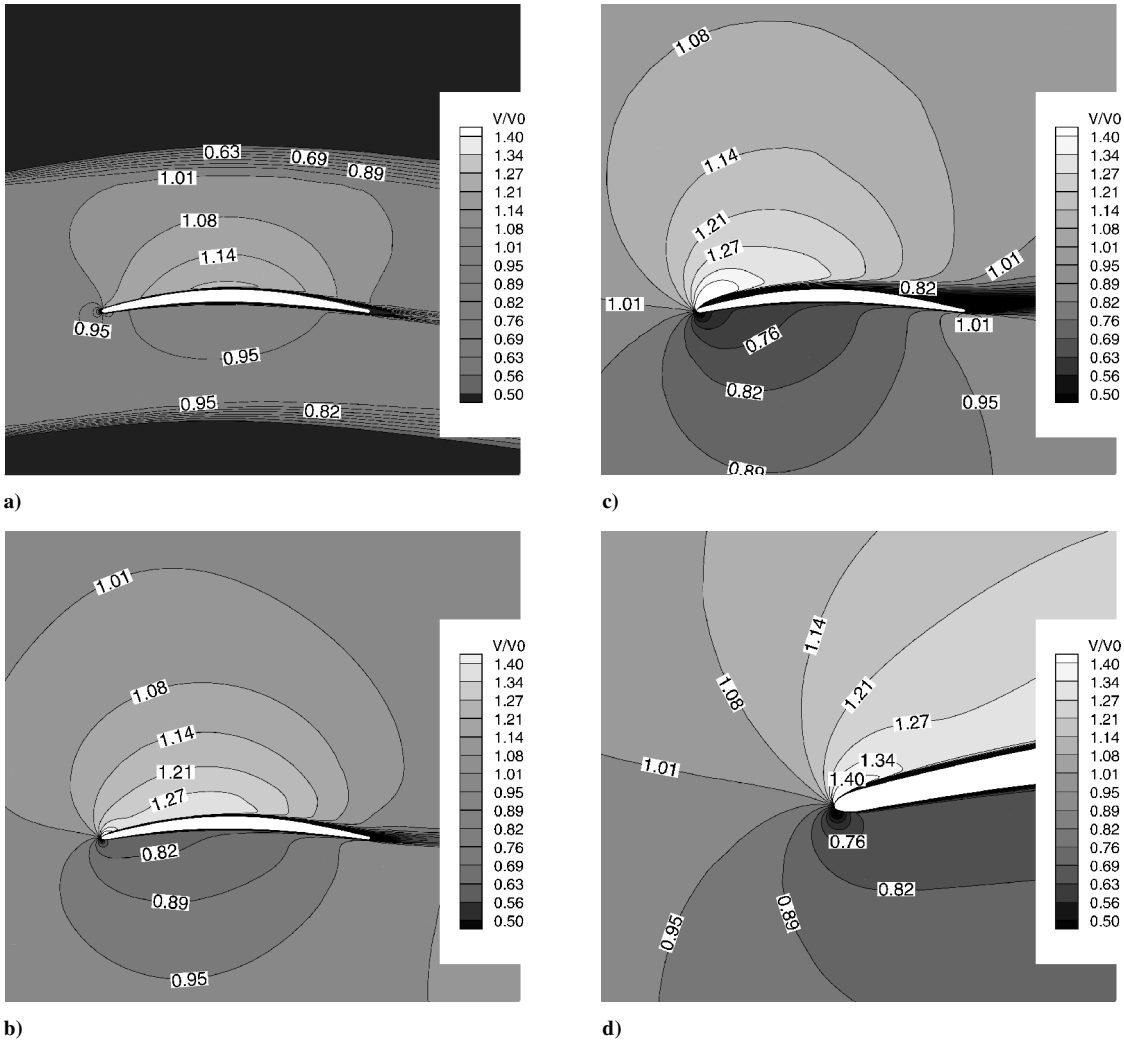

Fig. 16 Normalized mean velocity magnitude for free-jet flow over the CD airfoil at $\alpha_w = 8$ deg, with different jet widths: a) $w = 13$ cm, b) $w = 50$ cm, c) free air, and d) closeup view of case b ($w = 50$ cm) in the nose region.

between experimental results and wind-tunnel calculations suggests that reliable information for defining the boundary conditions of future LES computations of trailing-edge noise can be provided by RANS in the case of a wide nozzle.

The velocity contours of Figs. 16 also confirm the earlier cascade findings. With the current ECL setup, the finite jet width induces a loading on the blade that spreads over the whole chord as in the cascade case. The wider the jet becomes, the more forward the loading shifts and the closer it approaches the free-air value. However, even with a 50-cm jet width, there is no evidence of flow separation at the leading edge, as clearly shown in the closeup view of the velocity contours in Fig. 16d and the wall pressure distribution in Fig. 15.

V. Conclusions

Detailed RANS simulations of typical freejet wind-tunnel experiments on airfoils have shown strong effects of the jet on the aerodynamic loading and flow characteristics. When the jet width is not sufficiently large compared to the streamwise projected area of the airfoil (width-to-chord ratio of about 1), the airfoil behaves in a manner closer to a blade cascade than to an isolated airfoil. The significant modification of the lift distribution and flowfield can in turn affect the nature of the sound radiation. These effects have implications for the appropriate boundary conditions needed to conduct LES of open-jet aeroacoustic experiments and could be responsible for the discrepancies among some earlier experimental and computational studies, for example, the different boundary-layer thicknesses observed by Manoha et al.[13] To reproduce the experimental flow conditions accurately, freestream boundary conditions are not adequate (unless the jet is very wide). More realistic conditions based on experimental velocity profiles or RANS calculations should be imposed.

RANS simulations with the V2F and SST models compare more favorably with the measured pressure distribution on the Valeo CD airfoil than those with the k–ε model. Remaining differences are most likely due to the incoming flow conditions at the wind-tunnel nozzle outlet and particularly the local turbulence level that can modify the transition point on the suction side of the airfoil and consequently the flow separation at the trailing edge.

In addition to the full wind-tunnel simulation, a simpler computational model of the open-jet acoustic tunnel with an inlet velocity profile of variable width has also been devised. This configuration captures most of the experimental setup effects in open-jet facilities, particularly in the aft section of the airfoil, which is critical to trailing-edge noise. The simplified configuration allows for quick parametric studies of the dependence of flow conditions on the airfoil profiles and the angle of attack, which is particularly useful for the design of experiments as well as for RANS and LES simulations.

The knowledge and techniques developed through this study have been utilized in an ongoing LES of an open-jet airfoil self-noise experiment with jet width of 50 cm. As shown in the earlier RANS calculations, the flowfield in the wind-tunnel configuration deviates significantly from that of an isolated airfoil in uniform freestream. To account for this effect in the aeroacoustic analysis, the mean velocity profiles from the RANS calculation are used to define the boundary conditions for the LES, which is performed in a smaller domain within the core of the jet to save computational cost. This approach allows an accurate simulation of the experimental flow conditions and, hence, promotes the accuracy of noise computation.

References

[1]Blake, W. K., and Gershfeld, J. L., "The Aeroacoustics of Trailing Edges," *Frontiers in Experimental Fluid Mechanics*, edited by M. Gad-el-Hak, Springer-Verlag, Berlin, 1988, Chap. 10, pp. 457–532.

[2]Wright, S. E., "The Acoustic Spectrum of Axial Flow Machines," *Journal of Sound and Vibration*, Vol. 45, No. 2, 1976, pp. 165–223.

[3]Caro, S., and Moreau, S., "Aeroacoustic Modeling of Low Pressure Axial Flow Fans," AIAA Paper 2000-2094, July 2000.

[4]Glegg, S. A. L., Baxter, S. M., and Glendinning, A. G., "The Prediction of Broadband Noise from Wind Turbines," *Journal of Sound and Vibration*, Vol. 118, No. 2, 1987, pp. 217–239.

[5]Hubbard, H. H., and Shepherd, K. P., "Aeroacoustics of Large Wind Turbines," *Journal of the Acoustical Society of America*, Vol. 89, No. 6, 1991, pp. 2495–2507.

[6]Blake, W. K., "A Statistical Description of Pressure and Velocity Fields at the Trailing Edge of a Flat Strut," David Taylor Naval Ship Research and Development Center, DTNSRD Rept. 4241, Bethesda, MD, Dec. 1975.

[7]Brooks, T. F., and Hodgson, T. H., "Trailing Edge Noise Prediction from Measured Surface Pressures," *Journal of Sound and Vibration*, Vol. 78, No. 1, 1981, pp. 69–117.

[8]Fink, M. R., "Experimental Evaluation of Theories for Trailing and Incidence Fluctuation Noise," *AIAA Journal*, Vol. 13. No. 11, 1975, pp. 1472–1477.

[9]Wang, M., Lele, S. K., and Moin, P., "Computation of Quadrupole Noise Using Acoustic Analogy," *AIAA Journal*, Vol. 34, No. 11, 1996, pp. 2247–2254.

[10]Wang, M., "Computation of Trailing-Edge Noise at Low Mach Number Using Large-Eddy Simulation," *Annual Research Briefs—1998*, Center for Turbulence Research, Stanford Univ./NASA Ames Research Center, 1998, pp. 91–106.

[11]Manoha, E., Troff, B., and Sagaut, P., "Trailing-Edge Noise Prediction Using Large-Eddy Simulation and Acoustic Analogy," *AIAA Journal*, Vol. 38, No. 4, 2000, pp. 575–583.

[12]Wang, M., and Moin, P., "Computation of Trailing-Edge Flow and Noise Using Large-Eddy Simulation," *AIAA Journal*, Vol. 38, No. 12, 2000, pp. 2201–2209.

[13]Manoha, E., Delahay, C., Sagaut, P., Mary, I., Ben Khelil, S., and Guillen, P., "Numerical Prediction of the Unsteady Flow and Radiated Noise from a 3D Lifting Airfoil," AIAA Paper 2001-2133, May 2001.

[14]Ffowcs Williams, J. E., and Hall, L. H., "Aerodynamic Sound Generation by Turbulent Flow in the Vicinity of a Scattering Half-Plane," *Journal of Fluid Mechanics*, Vol. 40, 1970, pp. 657–670.

[15]Roger, M., and Moreau, S., "Trailing Edge Noise Measurements and Predictions for Subsonic Loaded Fan Blades," AIAA Paper 2002–2460, June 2002.

[16]Pérennès, S., "Caractérisation des Sources de Bruit Aérodynamique à Basses Fréquences de Dispositifs Hypersustentateurs," Ph.D. Dissertation No. 99-32, Laboratoire de Mécanique des Fluides et Acoustique, Ecole Centrale de Lyon, Ecully, France, 1999.

[17]Pérennès, S., and Roger, M., "Aerodynamic Noise of a Two-Dimensional Wing with High-Lift Devices," AIAA Paper 98-2338, July 1998.

[18]Knight, M., and Harris, T. A., "Experimental Determination of Jet Boundary Corrections for Airfoil Tests in Four Open Wind Tunnel Jets of Different Shapes," NACA Rept. 361, 1930.

[19]Moreau, S., and Bennett, E., "Improvement of Fan Design using CFD," Society of Automotive Engineers, Paper SAE-970934, Feb. 1997.

[20]Coggiola, E., Dessale, B., Moreau, S., and Broberg, R., "On the Use of CFD in the Automotive Engine Cooling Fan System Design," AIAA Paper 98-0772, Jan. 1998.

[21]Iaccarino, G., "Predictions of a Turbulent Separated Flow Using Commercial CFD Codes," *Journal of Fluid Engineering*, Vol. 123, 2001, pp. 1–10.

[22]Menter, F. R., "Two-Equation Eddy-Viscosity Turbulence Models for Engineering Applications," *AIAA Journal*, Vol. 32, No. 8, 1994, pp. 1598–1605.

[23]Durbin, P. A., "Separated Flow Computations with the k–ϵ–v^2 Model," *AIAA Journal*, Vol. 33, 1995, pp. 659–664.

[24]Winklemann, A. E., and Barlow, J. B., "A Flowfield Model for a Rectangular Platform Wing," *AIAA Journal*, Vol. 18, 1980, pp. 1006–1008.

[25]Bastedo, W. G., and Mueller, T. J., "Spanwise Variation of Laminar Separation Bubbles on Wings at Low Reynolds Numbers," *Journal of Aircraft*, Vol. 23, 1986, pp. 687–694.

[26]Henner, M., Stanciu, M., Moreau S., Aubert, S., and Ferrand, P., "Unsteady Rotor–Stator Interactions in Automotive Engine Cooling Fan Systems," *Proceedings of the ISUAAAT 2000 Conference*, edited by P. Ferrand and S. Aubert, PUG, 2000, pp. 570–579.

[27]Brooks, T. F., Marcollini, M. A., and Pope, D. S., "Airfoil Trailing-Edge Flow Measurements," *AIAA Journal*, Vol. 24, No. 8, 1986, pp. 1245–1251.

R. M. C. So
Associate Editor